Materials Research Bulletin 45 (2010) 1832–1836

Contents lists available at ScienceDirect

Materials Research Bulletin

journal homepage: www.elsevier.com/locate/matresbu

Photoluminescence and energy storage traps in $CaTiO_3:Pr^{3+}$

Xianmin Zhang [a,*], Chunyan Cao [b], Chenghua Zhang [a], Shiyao Xie [a], Guangwen Xu [a], Jiahua Zhang [c], Xiao-jun Wang [d,**]

[a] Department of Physics, Liaoning University, 66 Chong Shan Middle Road, Shenyang 110036, China
[b] College of Mathematics and Physics, Jinggangshan University, Ji'an 343009, China
[c] Key Laboratory of Excited State Processes, Chinese Academy of Sciences, Changchun 130033, China
[d] Department of Physics, Georgia Southern University, Statesboro, GA 30460, USA

ARTICLE INFO

Article history:
Received 24 February 2010
Received in revised form 31 July 2010
Accepted 14 September 2010
Available online 24 September 2010

Keywords:
A. Optical materials
C. X-ray diffraction
D. Defects
D. Energy storage

ABSTRACT

Red-emitting $CaTiO_3:Pr^{3+}$ phosphors are fabricated using a solid state method and structurally characterized by X-ray diffraction and field emission scanning electron microscopy. The optical properties are investigated using photoluminescence emission, excitation, photoluminescence decay curves, diffused reflectance and thermoluminescence spectra, and persistent phosphorescence decay curves. The optimal fabrication temperatures for photoluminescence and persistent phosphorescence are found at 1200–1300 °C for photoluminescence and 1400 °C for persistent phosphorescence. The energy storage traps for persistent phosphorescence in the system are analyzed based on the dependence of photoluminescence and persistent phosphorescence on sintering temperature. The distribution of energy storage traps is further characterized by thermoluminescence spectra and the parameters of the traps are calculated. Oxygen vacancies as the main trapping centers play the key role for persistent phosphorescence in $CaTiO_3:Pr^{3+}$.

1. Introduction

Red-emitting $CaTiO_3:Pr^{3+}$ phosphors have received extensive attention due to the excellent color purity and high chemical stability for various displays and signing applications [1–5]. Many researchers reported the enhancement of the photoluminescence [6–10] and persistent phosphorescence [11–13] with addition of different metal ions, such as Al^{3+}, Bi^{3+}, Zn^{2+} and Ln^{3+} (Ln = La, Lu, Gd). The solid solutions of (Ca, Sr) $TiO_3:Pr^{3+}$ [2,14] and (Ca, Sr, Ba) $TiO_3:Pr^{3+}$ [15] were also studied to explore the relationship between the structures and photoluminescence properties. It is clear that the red photoluminescence of $CaTiO_3:Pr^{3+}$ results from the transition of $^1D_2$–$^3H_4$ of Pr^{3+}. However, the nature of energy storage trapping centers proposed for the persistent phosphorescence in $CaTiO_3:Pr^{3+}$ is still a matter of controversy. Pan et al. ascribed the energy storage to the Pr^{3+} dopant itself as a hole-trapping center [3], while, Jia and the co-workers proposed the traps in $CaTiO_3:Pr^{3+}$ as oxygen vacancies and Pr^{4+}, which had the nature as an electron trap [4].

In this paper, the photoluminescence of $CaTiO_3:Pr^{3+}$ fabricated by a solid state method is studied using photoluminescence emission and excitation spectra and persistent phosphorescence decay curves as well as thermoluminescence (TL) spectra. The optimal fabrication temperatures for photoluminescence and persistent phosphorescence are studied for the first time. Our observations show oxygen vacancies as the main trapping centers play the key role for persistent phosphorescence in $CaTiO_3:Pr^{3+}$.

2. Experiment

The powders of $CaCO_3$, TiO_2 and $Pr(NO_3)_3$ solution were mixed in the de-ionized water, and then heated at 100 °C for 5 h to obtain the dried powders. The powders were ground in fume cupboard for 1 h until the pellets formed. The final samples were obtained after the pellets were sintered at different temperatures for 4 h in air. The dopant concentration of Pr^{3+} was fixed at 0.1 mol%.

The structural characterization was analyzed by X-ray diffraction (XRD; Rigaku D/max-rA) spectra with the Cu Kα line of 1.540 78 Å. The morphology of products was observed by field emission scanning electron microscopy (FESEM, Hitachi S-4800). Photoluminescence emission and excitation spectra, diffused reflectance spectra ($BaSO_4$ sample was used as a standard) and phosphorescence decay curves were measured using Hitachi F-4500 fluorescence spectrophotometer. Persistent phosphorescence were measured after irradiation by 375 nm ultraviolet (UV) light for 10 min. For lifetime measurement, the third (355 nm) harmonic of a Nd–YAG laser is used as the excitation source, and the signal is

* Corresponding author. Tel.: +86 24 62202305; fax: +86 24 62202305.
** Corresponding author.
E-mail addresses: xianmin596@sohu.com (X. Zhang), xwang@georgiasouthern.edu (X.-j. Wang).

0025-5408/$ – see front matter © 2010 Elsevier Ltd. All rights reserved.
doi:10.1016/j.materresbull.2010.09.022

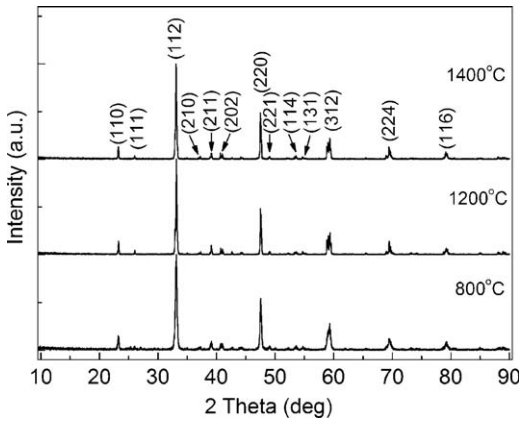

Fig. 1. XRD patterns of $CaTiO_3:Pr^{3+}$ sintered at different temperatures (800 °C, 1200 °C and 1400 °C).

detected with a Tektronix digital oscilloscope (TDS 3052). The TL spectra were recorded using a TL meter with a heating rate of 2 K/s.

3. Results and discussion

3.1. Microstructure characters: XRD and FESEM studies

XRD patterns of $CaTiO_3:Pr^{3+}$ sintered at various temperatures are shown in Fig. 1. The XRD pattern of these samples is consistent with the orthorhombic $CaTiO_3$ phase (JCPDS Card No. 82-0228). There is no appreciable difference in XRD peaks for the sample fabricated at 1200 °C compared to that at 1400 °C. The sample at 800 °C exhibits larger widths of the XRD peaks than the other two samples, which results from the poor crystallinity. Fig. 2 presents the corresponding FESEM images of the samples. It is found that the sample obtained at 800 °C has the size around 0.5–1.0 μm, consisting of the aggregates. The particle size increases to 2.0–4.0 μm for the sample fabricated at 1200 °C. The fused particles with size beyond 6.0 μm are observed for the sample prepared at 1400 °C.

3.2. Photoluminescence spectra of $CaTiO_3:Pr^{3+}$

The photoluminescence emission (λ_{ex} = 330 nm) and excitation (λ_{em} = 610 nm) spectra of $CaTiO_3:Pr^{3+}$ are presented in Fig. 3. The excitation spectra mainly consists of three broad bands in ultraviolet region, which are located at 265, 330 and 375 nm, respectively. The band at 265 nm corresponds to the absorption of Pr^{3+} 4f5d states [1,4]. The band located at 330 nm originates from the band edge absorption of $CaTiO_3$ host due to O(2*p*)-Ti(3*d*) transition [1] and the one at 375 nm is assigned to a low-lying Pr to-metal (Pr^{3+}–Ti^{4+}) intervalence charge transfer state [16]. The photoluminescence emission spectra show the red emission peaking at 610 nm is due to $^1D_2$–$^3H_4$ transition of Pr^{3+}. The photoluminescence decay curves are measured and presented in Fig. 4. The shortest lifetime of Pr^{3+} emission is observed for 800 °C sample. According to the previous report [17], some residual hydroxyl groups absorbed on the surface of powder particles can act as nonradiative centers for the quenching of Pr^{3+} emission when the sample was fabricated at low temperature. With increasing temperature, the number of hydroxyl reduces and leads to the increase of lifetime in $CaTiO_3:Pr^{3+}$. Herein, it is observed that the lifetime of Pr^{3+} emission is longer for the 1200 °C sample than that of the 800 °C. However, it is found that the lifetime of Pr^{3+} emission becomes shorter at 1400 °C than that of the 1200 °C, it is still longer compared to 800 °C sample though. More negatively charged defects, such as Ca vacancies [17,18] and/or Ti vacancies [4,14,16,17] and/or by reduction of Ti^{4+} to Ti^{3+} [17–21] formed in the $CaTiO_3$ host when the sintering temperature further increases (This will be discussed in detail by the diffused reflectance spectra of Fig. 5 in next paragraph). The extra charges can be compensated by forming the positively charged oxygen vacancies in the host [4,14,16]. The presence of oxygen vacancies in $CaTiO_3$ had also approved by a computer simulation study [22]. Several of these negatively charged defects (Ca and/or Ti vacancies, and/or Ti^{3+}) are undesirable because their presence in the phosphors can quench the Pr emission [9,17]. Therefore, it is expected that the lifetime decreases when the sintering temperature further increases to 1400 °C.

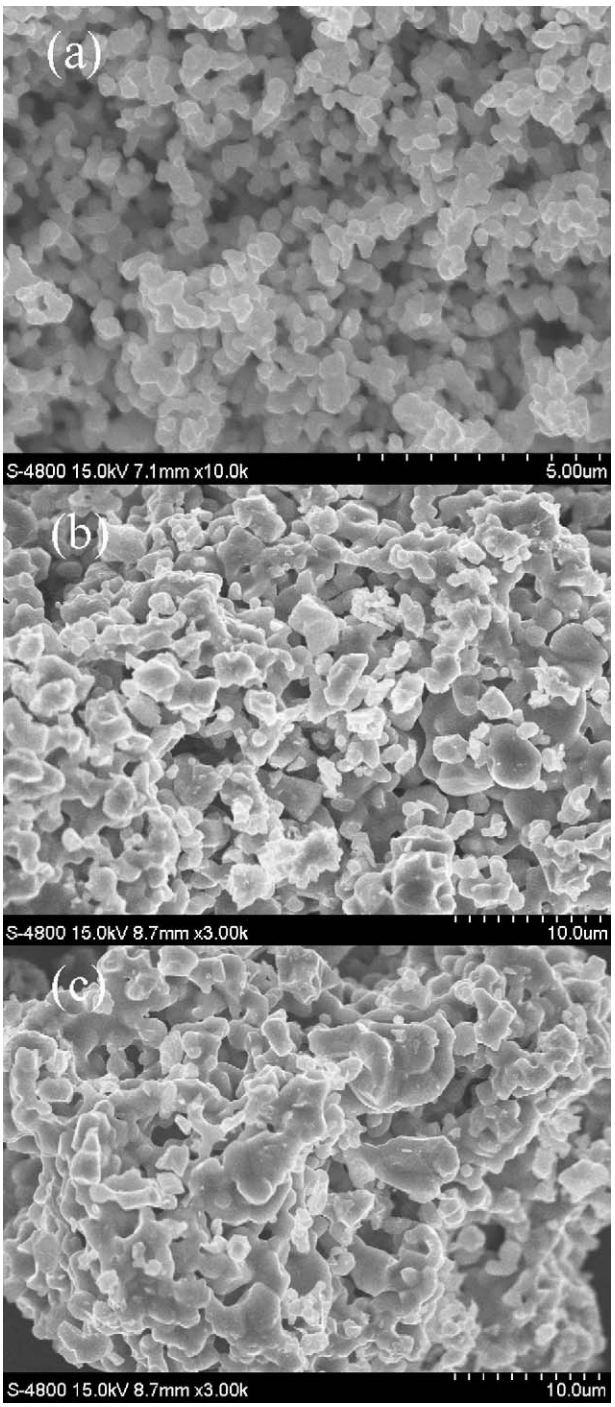

Fig. 2. The FESEM images of $CaTiO_3:Pr^{3+}$ fabricated at (a) 800 °C, (b) 1200 °C and (c) 1400 °C.

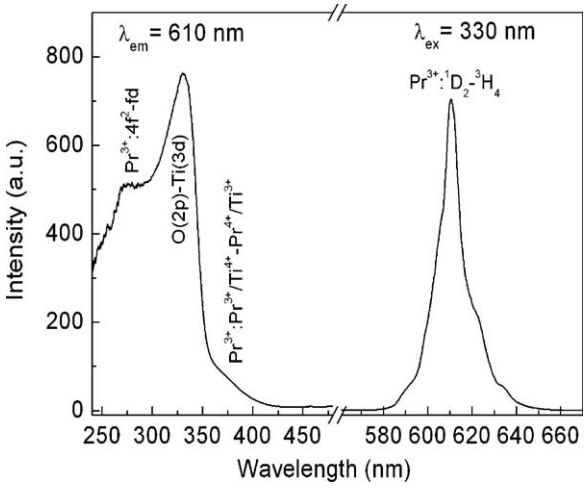

Fig. 3. Photoluminescence emission (λ_{ex} = 330 nm) and excitation spectra (λ_{em} = 610 nm) of $CaTiO_3:Pr^{3+}$.

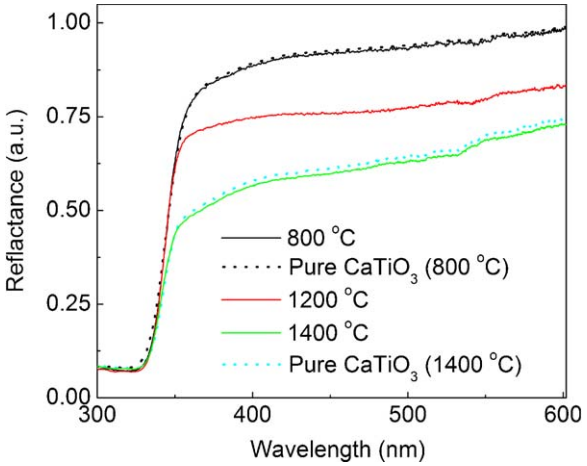

Fig. 5. Diffused reflectance spectra of $CaTiO_3:Pr^{3+}$ samples fabricated at different temperatures (800 °C, 1200 °C and 1400 °C). Dotted lines are pure $CaTiO_3$ samples for 800 °C and 1400 °C, respectively.

The diffused reflectance spectra are measured and provided in Fig. 5. One can find that the reflectance is obviously reduced with increasing sintering temperature. There are several kinds of negatively charged defects mentioned above in pure $CaTiO_3$ host, which can be compensated by positively charged oxygen vacancy. These defects acting as color centers can absorb the visible light. So it is very difficult to get a $CaTiO_3$ sample with pure white [4,9,15]. This is consistent with the observation of Fig. 5 where the reflectance of $CaTiO_3$ (dotted line) in visible light range is around 90% for 800 °C sample. With increasing temperature, the reflectance decreases to 60% for 1400 °C sample (dotted line) owing to the increase of color centers. Pr^{3+} is commonly admitted to locate in the Ca^{2+} site in $CaTiO_3:Pr^{3+}$ [1]. In addition, Pr^{3+} can be easily oxidized to Pr^{4+} when $CaTiO_3:Pr^{3+}$ was sintered in air [4,14,16]. The extra positive charges were likely compensated by some negatively charged defects mentioned above. This can be confirmed by the decrease of reflectance in $CaTiO_3:Pr^{3+}$ (solid line) compared to pure $CaTiO_3$ (dotted line), as shown in Fig. 5. Boutinaud pointed out that Pr^{4+} gave rise to yellow color of the phosphor due to the absorption in blue spectral range when $CaTiO_3:Pr^{3+}$ was sintered 430 h [16]. In Fig. 5, we did not observe prominent absorption from Pr^{4+} because all the samples are sintered only 4 h. It is shown that the reflectance of $CaTiO_3:Pr^{3+}$ (solid line) decreases with the increase of temperature due to the formation of the negatively charged defects and Pr^{4+}. Moreover, the change of body color for these phosphors is consistent with the decrease of reflectance. The sample color becomes darker and darker with the increase of temperature. The color is nearly white for 800 °C sample and becomes gray for 1400 °C sample. In the process, more oxygen vacancies formed in the host in order to compensate the extra negative charges. The formation of these oxygen vacancies as trapping centers will benefit to the phosphorescence in $CaTiO_3:Pr^{3+}$.

3.3. Persistent phosphorescence properties of $CaTiO_3:Pr^{3+}$

The time decay curves of persistent phosphorescence (λ_{em} = 610 nm) for $CaTiO_3:Pr^{3+}$ sintered at different temperatures is illustrated in Fig. 6. It is found the persistent phosphorescence intensity of the sample obtained at 1200 °C is lower in comparison with the 800 °C sample. The greatest persistent phosphorescence intensity is experimentally observed for the sample prepared at 1400 °C. The detailed relation of persistent phosphorescence intensities to annealing temperature will be discussed in next section. The inset of Fig. 6 represents the persistent phosphorescence spectra recorded at 100 s after the cessation of UV-light irradiation. The position and profile of the persistent phosphores-

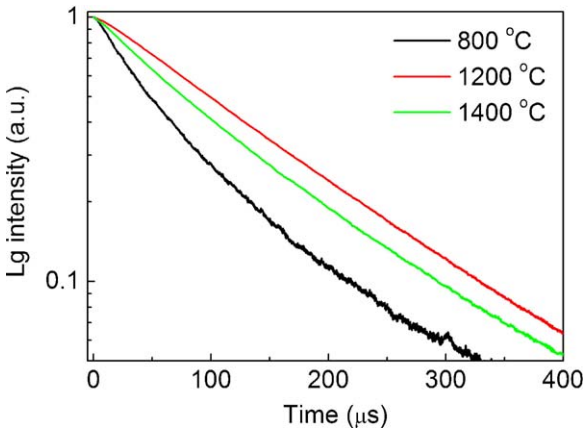

Fig. 4. Photoluminescence decay curves of the emission at 615 nm of $CaTiO_3:Pr^{3+}$ samples fabricated at different temperatures (800 °C, 1200 °C and 1400 °C).

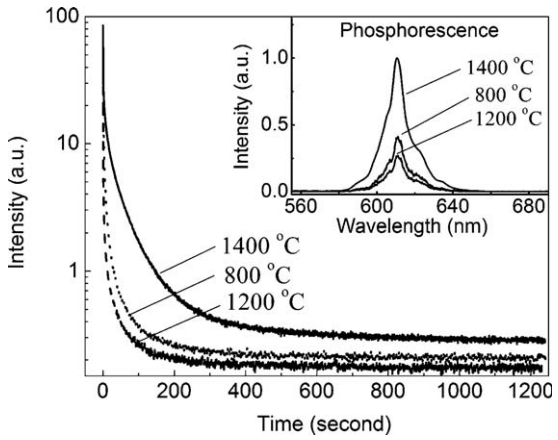

Fig. 6. Persistent phosphorescence (λ_{em} = 610 nm) decay curves of $CaTiO_3:Pr^{3+}$ fabricated at different sintering temperatures after irradiation by 375 nm UV-light for 10 min. Inset: the normalized phosphorescence spectra compared to 1400 °C sintered sample, which is recorded at 100 s after the cessation of UV-light irradiation.

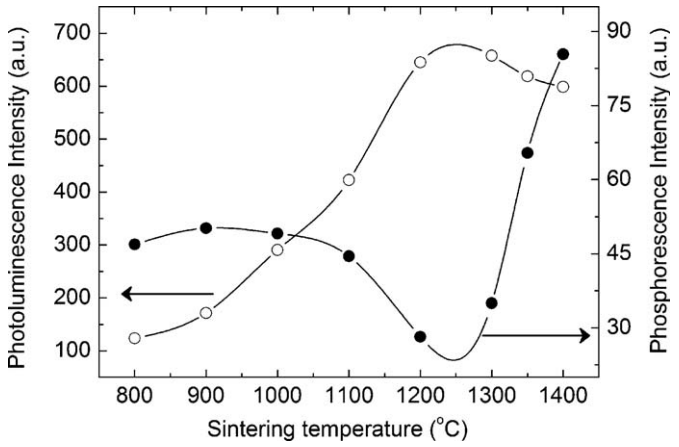

Fig. 7. Dependence of photoluminescence intensities (λ_{ex} = 330 nm) and persistent phosphorescence intensities (λ_{irra} = 375 nm) on annealing temperature in $CaTiO_3:Pr^{3+}$.

cence emission are consistent with the photoluminescence, indicating the persistent phosphorescence resulting from the $^1D_2$–$^3H_4$ transition of Pr^{3+}.

3.4. Dependence of photoluminescence and persistent phosphorescence on annealing temperature

The dependence of $CaTiO_3:Pr^{3+}$ photoluminescence intensity on annealing temperature is presented in Fig. 7. It is found the intensity increases with the increase of temperature from 800 to 1300 °C, which is characteristic in luminescent materials. As temperature increases, the number of nonradiative centers (hydroxyl groups) decreases and the lifetime of Pr^{3+} emission (Fig. 4) increases, intensifying the photoluminescence. In addition, the densification of the powders also contributes, to some extent, to the enhancement of photoluminescence [17]. Meanwhile, more Pr^{3+} should be oxidized to Pr^{4+} when $CaTiO_3:Pr^{3+}$ was sintered in air [4,17]. Consequently, the increase of lifetime and the decrease of the number of Pr^{3+} lead to the maximal photoluminescence when the samples treated in the range of 1200–1300 °C. Further increase of temperature above 1300 °C, more negatively charged defects [4,14,16–21] will be formed in the host (Fig. 5), which act as nonradiative centers and quench the Pr^{3+} emission (Fig. 4). The increase of Pr^{4+} can also reduce Pr^{3+} emission. Thus, the decrease of photoluminescence is observed for 1400 °C sample. The intensities of persistent phosphorescence as function of annealing temperature for these samples are also plotted in Fig. 7. It is observed that the persistent phosphorescence remains nearly unchanged from 800 °C to 1000 °C and begins to decrease from 1100 °C. It attains a minimum when the temperature is 1200 °C and then increases to a maximum at 1400 °C. The persistent phosphorescence intensity is proportional to the density of energy storage traps. The nature of energy storage trapping centers for the persistent phosphorescence in $CaTiO_3:Pr^{3+}$ has been attributed to different mechanisms, the Pr^{3+} dopant itself as a hole-trap and oxygen vacancies, Pr^{4+} as electron-traps, respectively [3,4]. With the increase of sintering temperature, more Pr^{3+} should be oxidized to Pr^{4+}. As a result, the persistent phosphorescence should monotonically reduce if Pr^{3+} dopant itself as the energy storage traps in $CaTiO_3:Pr^{3+}$. This is inconsistent with the experimental results as shown in Fig. 7. Based on the previous reports [4,17,22] and the results of Fig. 5, both oxygen vacancies and Pr^{4+} exist in $CaTiO_3:Pr^{3+}$. Thus, it is believed that the energy storage traps in $CaTiO_3:Pr^{3+}$ are associated with oxygen vacancies and Pr^{4+}.

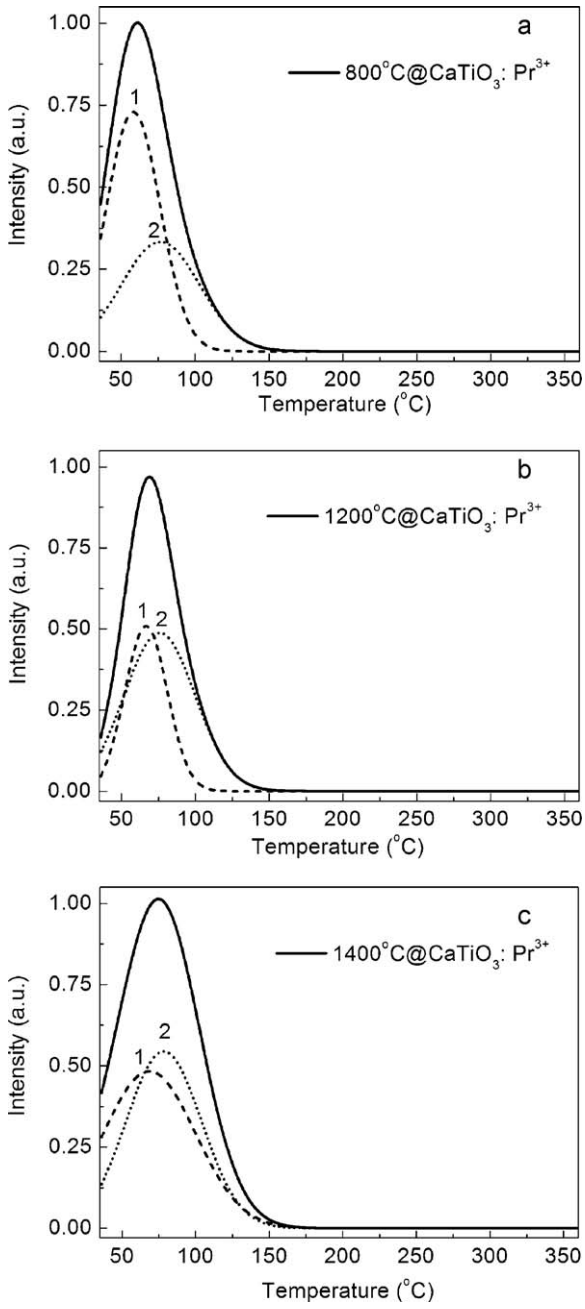

Fig. 8. Thermoluminescence spectra of $CaTiO_3:Pr^{3+}$ fabricated at different sintering temperatures: (a) 800 °C, (b) 1200 °C and (c) 1400 °C. The spectra were decomposed into curve 1 (dashed line) and curve 2 (dotted line) using two Gaussian fittings.

3.5. Thermoluminescence spectra in $CaTiO_3:Pr^{3+}$

To investigate the distribution of energy storage traps in $CaTiO_3:Pr^{3+}$, TL spectra are measured from room temperature to 360 °C, as plotted in Fig. 8. There is only one peak observed in the temperature range for all the samples. The TL peak shifts to the high temperature side with increasing fabrication temperature, from 62 °C of 800 °C fabricated sample to 68 °C and 76 °C for 1200 °C and 1400 °C fabricated samples, respectively. Meanwhile, the width of the TL peaks broadens as annealing temperature increases. The full width at half maximum (FWHM) of TL peak is 52 °C for the sample fabricated at 800 °C. This is broader than that of the sample obtained at 1200 °C (43 °C). The broadest FWHM of 68 °C is observed for the sample fabricated at 1400 °C. Considering

Table 1
Trap parameters of curve 1 and curve 2 for samples fabricated at different temperatures.

Fabrication temperature	Curve 1			Curve 2		
	T_m (K)	ω	E (eV)	T_m (K)	ω	E (eV)
800 °C	332	44	0.70	351	63	0.53
1200 °C	339	33	0.99	348	63	0.51
1400 °C	341	75	0.41	352	61	0.55

the two kinds of energy storage traps, oxygen vacancies and Pr^{4+}, the TL spectra were decomposed into two Gaussian curves, as depicted in Fig. 8. The depth of trap is estimated using the following equation given by Chen [23]

$$E = 3.5\left(\frac{kT_m^2}{\omega}\right) - 2kT_m$$

where E is the average depth of traps, T_m the peak temperature, ω the FWHM of the peak, and k the Boltzmann constant. The calculated results are listed in Table 1. Trap parameters of curve 1 (dashed lines) remarkably vary with increasing fabrication temperature. E is calculated to be 0.70, 0.99 and 0.41 eV for the samples fabricated at 800, 1200 and 1400 °C, respectively and ω is 44, 33 and 75 °C corresponding to the three samples. In contrast, the change of trap parameters of curve 2 (dotted lines) is negligible. E and ω remain the values of around 0.51 eV and 61 °C for all the samples. It is suggested that the traps related to curve 1 result from the oxygen vacancies, which is strongly dependent on the sintering temperature [16,17]. While the traps related to curve 2 are due to the Pr^{4+} since the low dopant concentration of Pr^{3+} (0.1 mol%) has limited effect on its distribution and density. Only can the traps formed with appropriate depths be expected to contribute to the persistent phosphorescence emission. The electrons stored in very deep traps cannot be thermally released under the temperatures for the TL study [24–26]. For the sample fabricated at 1400 °C, curve 1 reveals the broadest FWHM and the shallowest trap depth, indicating that the sample has the most energy storage traps suitable for persistent phosphorescence and the oxygen vacancies play the key role for trapping electrons.

The spectral measurements and calculations confirm that the energy storage traps in $CaTiO_3:Pr^{3+}$ are associated with both oxygen vacancies and Pr^{4+} dopants, but the oxygen vacancies play the key role for trapping electrons, which is well agreed with the experimental observation for the phosphorescence shown in Fig. 7. For the sample fabricated at 800 °C, oxygen vacancies with the middle depth (Table 1) and Pr^{4+} as trapping centers contribute to the persistent phosphorescence. As the annealing temperature increases, the energy storage traps (oxygen vacancies) becomes deeper. As a consequence, the persistent phosphorescence intensity is reduced. More oxygen vacancies with the shallower depth were formed to compensate the extra negatively charged defects in the host when the annealing temperature is above 1300 °C (Fig. 5). Thus, the enhancement of initial persistent phosphorescence intensity and persistent time (Figs. 6 and 7) is expected. Meanwhile, the increase of Pr^{4+} reduces the number of photoluminescence centers of Pr^{3+}. Some defects related to Ca and Ti vacancies formed in the host, as quenching centers, can further reduce the emission efficiency of $^1D_2$ of Pr^{3+} [9,17]. Herein, the decrease of photoluminescence is observed for 1400 °C sample, as shown in Fig. 7. For the temperature range in this experiment, the optimal fabrication temperatures are observed in the range of 1200 °C–1300 °C for photoluminescence and 1400 °C for persistent phosphorescence. It is expected that the decrease of photoluminescence and the increase of persistent phosphorescence may continue as annealing temperature increases above 1400 °C.

4. Conclusion

The $CaTiO_3:Pr^{3+}$ phosphors have been fabricated by a conventional solid state method and their optical properties are investigated. The optimal fabrication temperatures are 1200–1300 °C for photoluminescence and 1400 °C for persistent phosphorescence, respectively. Oxygen vacancies as the main electron trapping centers contribute the most for persistent phosphorescence emission in $CaTiO_3:Pr^{3+}$ system.

Acknowledgements

We thank Dr. Donghui Long for the help in spectral measurements. This work is financially supported by the National Natural Science Foundation of China (10847141), the Research Program of Liaoning Educational Department (2009A308), the Natural Science Foundation of Jiangxi Province (2009GQW0010) and Jiangxi Provincial Department of Education Science and Technology Program funded project (GJJ10203).

References

[1] P.T. Diallo, P. Boutinaud, R. Mahiou, J.C. Cousseins, Phys. Status Solidi A 160 (1997) 255.
[2] W. Jia, W. Xu, I. Rivera, Solid State Commun. 126 (2003) 153.
[3] Y.X. Pan, Q. Su, H.F. Xu, T.H. Chen, W.K. Ge, C.L. Yang, M.M. Wu, J. Solid State Chem. 174 (2003) 69.
[4] W. Jia, D. Jia, T. Rodriguez, D.R. Evans, R.S. Meltzer, W.M. Yen, J. Lumin. 119–120 (2006) 13.
[5] S. Okamotoa, H. Yamamotob, J. Lumin. 102–103 (2003) 586.
[6] J. Tang, X. Yu, L. Yang, C. Zhou, X. Peng, Mater. Lett. 60 (2006) 326–329.
[7] W. Jia, A. Perez-Andujar, I. Rivera, J. Electrochem. Soc. 150 (2003) H161.
[8] S.Y. Yin, D.H. Chen, W.J. Tang, J. Alloys Compd. 441 (2007) 327.
[9] X.M. Zhang, J.H. Zhang, X. Zhang, L. Chen, Y.S. Luo, X.J. Wang, Chem. Phys. Lett. 434 (2007) 237.
[10] W.J. Tang, D.H. Chen, Phys. Status Solidi A 206 (2009) 229.
[11] D. Haranath, A.F. Khan, H. Chander, J. Phys. D: Appl. Phys. 39 (2006) 4956.
[12] X.F. Yuan, X.B. Shi, M.R. Shen, W. Wang, L. Fang, F.G. Zheng, X.L. Wu, J. Alloys Compd. 485 (2009) 831.
[13] X.M. Zhang, J.H. Zhang, X. Zhang, L. Chem, S.Z. Lu, X.J. Wang, J. Lumin. 122–123 (2007) 958.
[14] P. Boutinaud, L. Sarakha, E. Cavalli, M. Bettinelli, P. Dorenbos, R. Mahiou, J. Phys. D: Appl. Phys. 42 (2009) 045106.
[15] T. Kyomen, R. Sakamoto, N. Sakamoto, S. Kunugi, M. Itoh, Chem. Mater. 17 (2005) 3200.
[16] P. Boutinaud, E. Pinel, M. Dubois, A.P. Vink, R. Mahiou, J. Lumin. 111 (2005) 69.
[17] P.T. Diallo, K. Jeanlouis, P. Boutinaud, R. Mahiou, J.C. Cousseins, J. Alloys Compd. 323–324 (2001) 218.
[18] L.S. Cavalcante, V.S. Marques, J.C. Sczancoski, M.T. Escote, M.R. Joya, J.A. Varela, M.R.M.C. Santos, P.S. Pizani, E. Longo, Chem. Eng. J. 143 (2008) 299.
[19] N.J. Cockroft, J.C. Wright, Phys. Rev. B 45 (1992) 9642.
[20] E.R. Vance, R.A. Day, Z. Zhang, B.D. Begg, C.J. Ball, M.G. Blackford, J. Solid State Chem. 124 (1996) 77.
[21] D. Makovec, Z. Samardzija, D. Kolar, J. Solid State Chem. 123 (1996) 30.
[22] M. Callejia, M.T. Dove, E.K.H. Salje, J. Phys.: Condens. Matter 15 (2003) 2301.
[23] R. Chen, J. Appl. Phys. 40 (1969) 570.
[24] T. Matsuzawa, Y. Aoki, N. Takeuchi, Y. Murayama, J. Electrochem. Soc. 143 (1996) 2670.
[25] J. Qiu, K. Miura, H. Inouye, Appl. Phys. Lett. 73 (1998) 1763.
[26] D. Jia, R.S. Meltzer, W.M. Yen, W. Jia, X. Wang, Appl. Phys. Lett. 80 (2002) 1535.